ELSEVIER

Contents lists available at SciVerse ScienceDirect

Optics Communications

journal homepage: www.elsevier.com/locate/optcom



A high temperature sensor based on a peanut-shape structure Michelson interferometer

Di Wu, Tao Zhu*, Min Liu

Key Laboratory of Optoelectronic Technology & Systems (Ministry of Education), Chongqing University, Chongqing 400044, China

ARTICLE INFO

Article history:
Received 10 January 2012
Received in revised form
25 June 2012
Accepted 26 June 2012
Available online 23 August 2012

Keywords: Fiber-optic sensor High temperature Michelson interferometer

ABSTRACT

A fiber temperature sensor with high sensitivity based on a Michelson interferometer is realized by fusion-splicing a peanut-shape structure in single-mode fiber (SMF). The theory and experimental results show that the peanut-shape structure can couple the light energy of the core mode into the cladding and re-couple the light in the cladding into the core. A high-quality interference spectrum with a fringe visibility of about 18 dB is observed. Experimental demonstration shows that the device can be heated up to $900\,^{\circ}\text{C}$ with a sensitivity of about $\sim 0.096\,\text{nm}/^{\circ}\text{C}$. The device has the advantages of low-cost, high sensitivity and easy fabrication, which makes it attractive for sensing applications.

© 2012 Elsevier B.V. All rights reserved.

1. Introduction

Optical fiber-based devices have many advantages for temperature sensing due to their lightweight, compact and resistant to electromagnetic interference. Long period fiber grating (LPFG) exhibits higher temperature sensitivity (\sim 0.1 nm/ $^{\circ}$ C) and low back reflection. However, since the excited cladding modes propagate in the cladding and the length of the LPFG is long (about 30-40 mm), the LPFG has high bending sensitivity which may limit the system operation flexibility [1,2]. Fiber Bragg grating (FBG) is particularly attractive for distributed sensing, but exhibits poor stability within the high-temperature environment and the grating can be completely erased at temperatures around 700 °C [3]. In particular, Canning et al. demonstrated a regenerated FBG which could be heated up to 1295 °C [4] and Zhang et al. proposed a hydrogenloaded FBG whose highest erasing temperature could reach to 1100 °C [5]. However, they suffer from limited temperature sensitivity of about ~ 0.01 nm/°C. Compared to the fiber grating based temperature sensors, the fiber interferometric sensors have the advantages of easy manufacture and good thermal stability. Wei et al. made a fiber inline Fabry-Perot interferometer (FPI) with a femtosecond laser for sensing applications in high temperature environments [6]. Zhu et al. demonstrated a fiber-optic FPI as a high-temperature sensor up to 1200 °C by using a special all-silica photonic crystal fiber [7]. Li et al. demonstrated a SMF/multimode fiber hybrid structure to form a Michelson fiber interferometer for temperature measurement up to 750 °C with the sensitivity of

 \sim 0.015 nm/°C [8]. Wang et al. reported a high temperature sensor based on an optical microfibre coupler, which could be heated up to 1000 °C [9]. Recently, the fiber in-line Mach-Zehnder interferometers (MZIs) based on the guided modes of the fiber, including fiber tapers, SMF, multimode fiber (MMF), twin-core fiber (TCF) and photonic crystal fiber (PCF) have been proposed for temperature measurement [8-14]. The MZI usually contains two cascaded fiber components which are used as the beam splitter and the combiner. The splitter couples the part energy of the core mode into the cladding modes, and the combiner recombines the cladding modes into the core, except for the TCF based MZI. The commonly used splitters/combiners include fiber tapers, LPFGs, the sections of MMF, TCF or PCF. However, LPFGs-based MZIs need a complex fabrication process, the fiber tapered MZIs have a degraded mechanical strength due to the small waist diameter and the MZIs with a section of special fiber have a high cost.

It is noticed that Li et al. proposed a MZI fabricated by fusion-splicing two ultra-abrupt fiber tapers as the beam splitter and combiner [15], where the ultra-abrupt tapered structure decreases the mode field of light rapidly. However, the ultra-abrupt fiber tapers have a degraded mechanical strength due to the small waist diameter, so it is perturbed easily by external environment; hence the excited cladding modes will be unsteady for the structure. In this paper, we used higher arc power level to fabricate a peanut-shape structure, which could enlarge the mode field diameter and decrease the insertion loss because of the lens effect of the structure. Since the Michelson interferometer only need an identical peanut-shape structure to be used as the splitter and combiner, it will have better performance than the MZI consisting of two peanut-shape structures. Due to the large difference of the thermal coefficients of the core mode and the

^{*} Corresponding author. Tel.: +86 023 6511 1973. E-mail address: zhutao@cqu.edu.cn (T. Zhu).

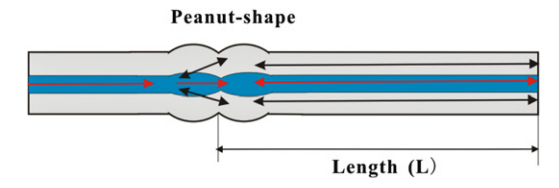


Fig. 1. Schematic diagram of the Michelson interferometer temperature sensor.

cladding modes, the proposed Michelson interferometer has higher temperature sensitivity ($\sim\!0.096~\text{nm}/^\circ\text{C}$). Meanwhile, the measured maximum strain of the peanut-shape structure is around $\sim\!3600~\mu\text{E}$, which makes it very robust and easy to be packed.

2. Principle

Fig. 1 shows the structural diagram of the Michelson interferometer. The input optical signal is split into two optical paths at the peanut-shape structure, along the core and the cladding of the fiber respectively, and then is recombined together when it is reflected back from the end surface (the end surface served as a mirror). Due to the phase difference between the core and the cladding modes, the Michelson interferometer could be used to measure many environmental parameters. The relative phase difference of the interfering two modes could be described as

$$4\pi (n_{eff}^{co} - n_{eff}^{cl,m}) \frac{L}{\lambda_N} = (2N+1)\pi \tag{1}$$

where n_{eff}^{co} is the effective index of the core mode, $n_{eff}^{cl,m}$ is the effective index of the mth cladding mode, L is the length between the peanut-shape structure and the end surface of fiber, λ_N is the center wavelength of the interference valley of the Nth order, and N is an integer. Thus, the temperature sensitivity of the Michelson interferometer can be calculated by

$$\frac{d\lambda_N}{dT} \approx 2\lambda_N \left[\frac{1}{n_{eff}^{co} - n_{eff}^{cl,m}} (\frac{dn_{eff}^{co}}{dT} - \frac{dn_{eff}^{cl,m}}{dT}) + \frac{1}{L} \frac{dL}{dT} \right]$$
 (2)

We use the standard SMF (Corning SMF-28) to fabricate the sensor, and the core of the fiber has a higher thermo-optic coefficient $(6.65 \times 10^{-6} \, ^{\circ}\text{C}^{-1})$ than that of the cladding $(6.50 \times 10^{-6} \, ^{\circ}\text{C}^{-1})$ [16]; hence the spectrum will move to the longer wavelength when the environment temperature increases.

3. Sensor fabrication

In the fabrication process, a high-accuracy optical spectrum analyzer (OSA, Si720, Micro Optics, USA) was used to monitor the interference spectrum of the sensor with a wavelength resolution and precision of 0.25 pm and 1 pm, respectively. A Furukawa S176 arc fusion splicing machine was used to fabricate the sensors.

Firstly, two sections of SMF were treated with proper arc discharge to fabricate the ellipsoidal microlens (as shown in Fig. 2(a)). The details of the arc discharge processing strategy are as follows: the arc power was $\sim\!200$, the pre-fuse time was $\sim\!170$ ms, and arc duration was $\sim\!1200$ ms. Since the arc power level of 200 was much higher than that of the arc power used in the standard SMF fusion splicing (100), the fiber end will become an ellipsoidal microlens. Also, Fan et al. fabricated a microspherical tip on an optical fiber by using the same method of large discharge power [17]. The parameters of the two fabricated ellipsoidal microlens (as shown in Fig. 2(a)) are $Z_1\!=\!200\,\mu\text{m}$, $Z_2\!=\!191\,\mu\text{m}$, and $R\!=\!207\,\mu\text{m}$. We used the beam propagation

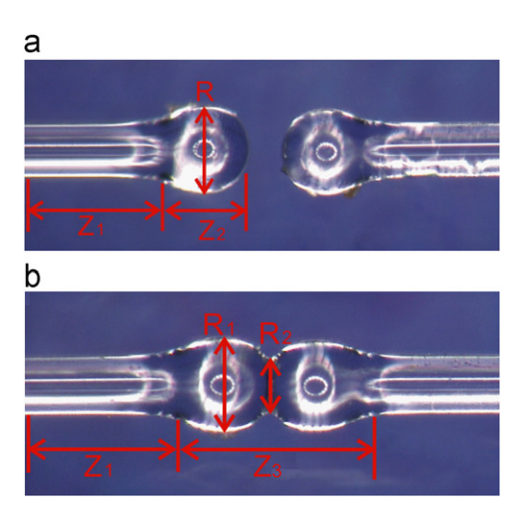


Fig. 2. Microscopic image of the peanut-shape structure: (a) after the arc discharge treatment and (b) after the fusion splicing.

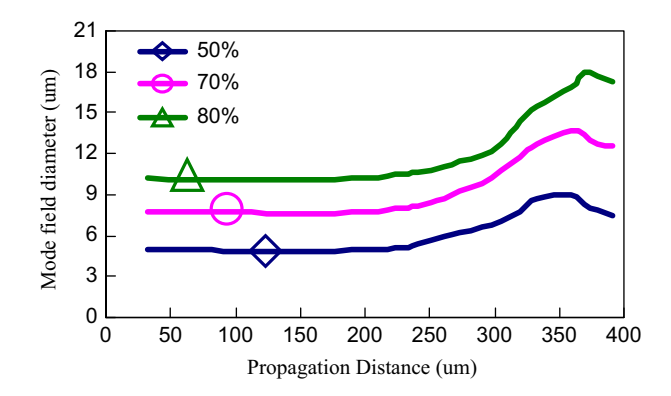


Fig. 3. Simulated mode field distribution along the ellipsoidal microlens: the mode field diameter of the 50% (a), 70% (b) and 80% (c) of total energy.

method (BPM) [18] to simulate the mode field distribution along the ellipsoidal microlens. As shown in Fig. 3, the mode field remains constant before it enters the ellipsoidal-structure section (Z_2), but increases as the propagating distance increases to 350 μ m. However, it begins to decrease when the propagation distance is farther than 350 μ m. This means that the light could be diverged at first and then be condensed later by the microlens. In general, 50%, 70% and 80% of the total energy will lead to the increase of mode field diameter from 5.00 μ m to 7.45 μ m, from 7.74 μ m to 12.51 μ m, and from 12.51 μ m to 17.23 μ m, respectively.

Although the ellipsoidal microlens can diverge the light, there was only a little energy of the core coupled into the cladding by the ellipsoidal microlens. So, we spliced two ellipsoidal microlenses to form a peanut-shape structure (as shown in Fig. 2(b)) to increase the power of the mode field in the cladding. It is noticed that the mode field of the light was increased at first by the peanut-shape structure, which is not like the ultra-abrupt fiber taper (the mode field was decreased rapidly at first). Thus, the peanut-shape structure could better diffuse the mode field and has lower loss than the ultra-abrupt fiber taper [15]. The parameters of the peanut-shape structure are as follows: R_1 =108 μ m, R_2 =207 μ m, Z_1 =200 μ m, and Z_3 =334 μ m. The used arc power level was 100, and the insertion loss of the peanut-shape structure was \sim 3 dB.

Since the peanut-shape structure could be used as the splitter or combiner, we used a single peanut-shape structure to form a Michelson interferometer instead of two to construct a MZI. Fig. 4(a) and (b) shows the interference spectra of the Michelson

Download English Version:

https://daneshyari.com/en/article/1536502

Download Persian Version:

https://daneshyari.com/article/1536502

<u>Daneshyari.com</u>